Available online at www.sciencedirect.com
ScienceDirect
Proceedings of the Combustion Institute 33 (2011) 309–316
Proceedings of the Combustion Institute
www.elsevier.com/locate/proci

A new shock tube study of the $H + O_2 \rightarrow OH + O$ reaction rate using tunable diode laser absorption of H_2O near 2.5 μm

Z. Hong *, D.F. Davidson, E.A. Barbour, R.K. Hanson

Department of Mechanical Engineering, Stanford University, Stanford, CA 94305, USA

Available online 19 September 2010

Abstract

The rate coefficient of the reaction $H + O_2 \rightarrow OH + O$ was determined using tunable diode laser absorption of H_2O near 2.5 μm behind reflected shock waves over the temperature range 1100–1530 K, at approximately 2 atm. Detailed kinetic analysis of the recorded H_2O temporal profiles yielded the rate coefficient expression: $k = (1.12 \pm 0.08) \times 10^{14} \exp[(-7805 \pm 90)/T]\ \mathrm{cm^3\ mol^{-1}\ s^{-1}}$, with estimated uncertainties of ±4.6% at 1500 K and ±8.8% at 1100 K. Excellent agreement between this study and that of Masten et al. (1990) was found in the overlapping temperature range. By combining the results of these two studies, the reaction rate coefficient over the range 1100–3370 K was found to be described well by:

$$k = (1.04 \pm 0.03) \times 10^{14} \exp[(-7705 \pm 40)/T]\ \mathrm{cm^3\ mol^{-1}\ s^{-1}}.$$

Keywords: Laser absorption; Shock tube; Hydrogen; Tunable diode laser

1. Introduction

The chain branching reaction between atomic hydrogen and molecular oxygen $H + O_2 \rightarrow OH + O$ (Rxn. 1) is one of the most important elementary reactions in combustion and has been the subject of many experimental studies and reviews [1–14].

In 1973, Schott [3] inferred the rate coefficient of this reaction (k_1) from chemiluminescence measurements of O–CO recombination in shock heated $H_2/CO/O_2/Ar$ mixtures at temperatures of 1250–2500 K. For many years Schott's approach appeared to be the most direct and his results were heavily weighted in the subsequent review by Warnatz [15]. In the decade following publication of the early reviews [15,16], more quantitative and direct diagnostics methods were adopted to investigate k_1. Atomic resonance absorption spectroscopy (ARAS) was used to monitor the time-histories of atomic hydrogen [5,7,8] or atomic oxygen concentrations [4,5] and other groups [6,9–14] applied CW ring-dye laser absorption spectroscopy techniques to measure OH radical time-history profiles and derive the rate coefficient of this reaction.

At temperatures above 1500 K, k_1 was mainly determined from OH time-histories in shock-heated $H_2/O_2/Ar$ mixtures. Despite similarities in

* Corresponding author. Address: Room 520I, Build 520, Mechanical Engineering Department, Stanford University, Stanford, CA 94305 USA. Fax: +1 (650) 723 1748.
E-mail address: hongzk@stanford.edu (Z. Hong).

1540-7489/$ - see front matter © 2010 The Combustion Institute. Published by Elsevier Inc. All rights reserved.
doi:10.1016/j.proci.2010.05.101

the experiments, discrepancies among the early studies [5,6,9,13] are as high as a factor of two at 2000 K. Subsequent studies helped to resolve these discrepancies. Yu et al. [13] reanalyzed the OH data from a previous study by Yuan et al. [10] and recovered results that supported the measurements of Masten et al. [9]. Yang et al. [12] suspected that there were air leaks in the shock tube in the previous k_1 study from the same laboratory [6] and reinvestigated the rate with another shock tube. Their new results again coincided with the rate expression given Masten et al. [9]. Du and Hessler [11] extended the measurements of k_1 to temperatures as high as 5300 K and again confirmed the results in Ref. [9]. The more recent study by Ryu et al. [14] and by Hwang et al. [17] obtained almost identical k_1 values of the previous researchers [9–13] over the range 1500–2500 K using laser absorption spectroscopy of OH radical.

At lower temperatures ($T < 1500$ K), however, disagreement still exists among the reported values [4,7,8,14,17]. At 1100 K, k_1 from Pamidimukkala et al. [4] is approximately 65% of the rate coefficients recommended by other researchers [8,14]. The determinations of k_1 at temperatures lower than 1500 K relied heavily on the ARAS method [4,7,8], and these measurements typically resulted in relatively large scatter (16% and 27% as reported in Refs. [7,8], respectively). In contrast, measurements using OH laser absorption [14,17] yield much smaller scatter in the inferred k_1 values (e.g., 6% as reported in Ref. [14]). However, at lower temperatures, it is difficult to accurately determine k_1 from OH profiles due to complications discussed later in the paper. As pointed out by Hwang et al. [17], a factor of 1.3 discrepancy exists between the two methods [7,14] at 1050 K. An alternative approach of examining k_1 with smaller scatter and better accuracy is desired at temperatures below 1500 K.

Tunable diode laser absorption spectroscopy of H_2O near 2.5 μm has recently been successfully employed to study the thermal decomposition rate of H_2O_2 behind reflected shock waves [18]. Using the same H_2O diagnostic method, simulations using the detailed chemical kinetics model GRI-Mech 3.0 [19] and the Senkin [20] kinetics code show that k_1 can be very accurately determined using the maximum slope of H_2O profiles in very dilute fuel-rich $H_2/O_2/Ar$ reflected shock wave experiments.

Here we present measurements of k_1 for temperatures of 1100–1500 K using the new H_2O diagnostic method developed in this laboratory. We also provide a comparison with previous studies of this reaction and review the influence that improved measurements [21] of the rate coefficient of reaction (2) $H + O_2 + M \rightarrow HO_2 + M$ and the enthalpy of formation of OH [22,23] have on k_1.

2. Experimental setup

Experiments were carried out in a high-purity, 304 stainless steel shock tube with inner diameter of 14.13 cm. The driven section of the shock tube is 8.54 m long, and the driver is 3.35 m long. A detailed description of the shock tube can be found in a previous study [18]. The temperatures behind the incident and reflected shocks, which are denoted as T_2 and T_5 respectively, were calculated using the normal shock equations. Uncertainty in T_5 at time zero is ±0.8% [24], resulting primarily from uncertainty in the measured incident shock velocity.

Compared to the uncertainty in initial T_5, temperature variations at longer test times can result in a larger uncertainty in k_1. Non-ideal flow effects in shock tubes, such as boundary layer growth, finite diaphragm-opening time, etc. can be responsible for the pressure and temperature variations seen at longer times [25]. For the shock tube used in this study, a typical pressure rise rate of 2%/ms is seen near the end section. The test time needed for H_2 oxidation at the fuel concentrations of the current study near 1100 K is 5 ms, therefore the departure from the usual constant U–V model could be as high as 25 K by the time the plateau level of H_2O is reached.

To reduce (or eliminate) effects of the facility-related increase in pressure and temperature behind reflected shock waves, the shock tube was modified by inserting a cone-shaped obstacle into the driver section [25]. Expansion waves reflected from the surface of the driver insert continuously propagate downstream into the driven section. The gentle decrease in pressure caused by these expansion waves is superimposed on the slow pressure rise related to the boundary layer growth, effectively eliminating the change in pressure and temperature. Uniform pressure profiles obtained in experiments are shown in Section 3.

Test gas mixtures were prepared manometrically (MKS Baratron capacitance manometer) in a stainless steel mixing tank equipped with a magnetic stirrer and turbomolecular pump. Research-grade gases (99.999%) supplied by Praxair were used. The Baratron has a precision better than 0.01 Torr for pressures under 100 and 0.1 Torr for greater pressures. Following the double dilution procedure, two test gas mixtures were prepared: 0.1% O_2, 0.9% H_2, balance Ar for tests at higher temperature (1250–1500 K), and 0.1% O_2, 2.9% H_2, balance Ar for tests at lower temperatures (1100–1250 K). The relative uncertainty in the test mixture compositions is less than 1%.

The water concentration histories were measured using tunable diode laser absorption of water at 2550.96 nm (3920.09 cm^{-1}) within the v_3 fundamental vibrational band. This transition was selected because of its large line strength

and lack of overlap with neighboring lines. The closest water feature is negligibly small and 1.5 cm^{-1} away from the line center.

For the selected water transition the line strength at 296 K was characterized in a static cell (0.6395 cm^{-2}/atm) and found to be in excellent agreement with the HITRAN [26] database. The collisional broadening coefficients (γ, half-width at half-maximum) of nitrogen and argon were also measured in separate cell and reflected shock experiments. Details of the H_2O absorption line characterization have been provided in a previous study [18]. Under typical experimental conditions ($P = 1100$ K, $T = 2$ atm), a peak absorbance of approximately 14% is expected with 2000 ppm of H_2O in Ar over a pathlength of 14.13 cm.

A distributed feedback (DFB) diode laser near 2.5 μm from Nanoplus GmbH was used. The laser wavelength and intensity were controlled by a combination of temperature and injection current using commercial controllers (ILX Lightwave LDT-5910B and LDX-3620). The laser wavelength was fixed at the center of the water absorption feature. The typical operating condition for the laser is 20.8 C and 90 mA, with intensity noise 0.01% rms.

The laser beam was collimated by a plano-convex lens, and transmitted through a pair of sapphire windows located 2 cm from the shock tube end wall. The beam was then passed through a Spectrogon narrow band-pass filter (center 2585 nm, half width: 35 nm), and finally focused by a plano-convex lens into an integrating sphere (SphereOptics SPH-1G-3) and detected by a liquid nitrogen-cooled InSb detector (IR Associates IS-2.0, 1 MHz bandwidth). The laser beam path was purged with pure N_2.

3. Results

Typical reflected shock wave pressure and laser transmission profiles are shown in Fig. 1. The data sets in the upper panel (Fig. 1a) were obtained in a 0.1% O_2/0.9% H_2/Ar mixture at initial conditions of 1472 K and 1.83 atm, close to the high-temperature limit of the current data. The temporal profiles presented in the lower panel (Fig. 1b) were acquired using a 0.1% O_2/2.9% H_2/Ar mixture at 1100 K and 1.95 atm, which is close to the low-temperature limit of the current study. The use of the larger H_2 concentration at low temperatures reduced the ignition delay times and does not affect k_1 determinations.

Figure 1 illustrates features common to all experiments in this study. After an initial period when chain carrier radials (H, O, and OH) were being accumulated, light absorption increased rapidly due to the formation of H_2O until a chemical partial equilibrium is achieved. Extremely uniform pressure profiles were obtained with the

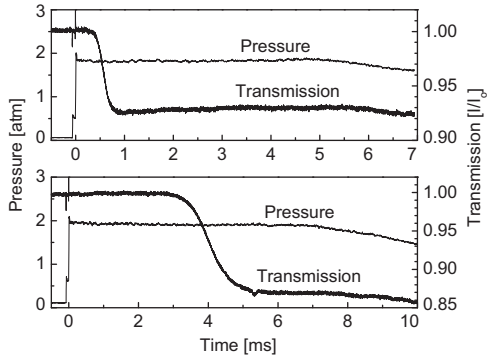

Fig. 1. Typical pressure and laser transmission histories in reflected-shock experiments: (a. upper) 0.1% O_2, 0.9% H_2, 99% Ar, 1472 K, 1.83 atm; (b. lower) 0.1% O_2, 2.9% H_2, 97% Ar, 1100 K, 1.95 atm.

driver inserts. Over the entire course of H_2 oxidation, at 1100 K (Fig. 1b) approximately 7 ms, the pressure fluctuation was less than ±1.5%, and the estimated long-time temperature uncertainty is less than ±0.6%, or ±6.7 K. The initial temperature was determined from the measured incident shock speed and the associated uncertainty was estimated to be ±7.7 K. The combined uncertainty in temperature for this low temperature example is ±10.2 K. For $T = 1472$ K (Fig. 1a), the combined temperature uncertainty is smaller (±9.4 K), since the test time needed is shorter for higher temperature ignition.

The mixtures were selected with the aid of computer simulations using a detailed chemical kinetic mechanism and the Senkin [20] kinetics code, with the aim of maximizing the sensitivity of the H_2O growth to k_1. To be consistent with our previous studies [18,27,28], an updated version of GRI-Mech 3.0 [19] was chosen to perform analyses in the current study. The updates to GRI-Mech 3.0 include the latest data for the OH heat of formation [22,23], the HO_2 heat of formation [29], the rate coefficients for the reactions $OH + HO_2 \rightarrow H_2O + O_2$ [27] and $OH + H_2O_2 \rightarrow H_2O + HO_2$ [28], and the rate constants of H_2O_2 thermal decomposition [18,28]. The choice of the base mechanism for analyzing experiment data only has minor effects on the determination of k_1, as will become evident in later analyses and discussions. Figure 2a shows the H_2O sensitivity analysis for the conditions of Fig. 1a. The analysis indicates that formation of H_2O is predominately controlled by the title reaction of $H + O_2 \rightarrow OH + O$. Only very small sensitivities are shown to the reactions $OH + H_2 \rightarrow H + H_2O$ (k_3) and $O + H_2 \rightarrow H + OH$ (k_4).

H_2O concentration time-histories were calculated from the attenuated laser beam transmissions (I/I_o) using Beer's law. The plateau H_2O level does not depend on the reaction kinetics

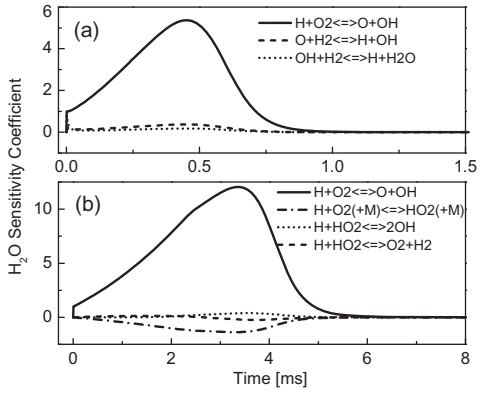

Fig. 2. H_2O sensitivity plot at conditions of the corresponding panels of Fig. 1.

but is determined by a chemical partial equilibrium. Typical discrepancies between the experimental observations and the numerical simulations were less than 1%. The slight mismatch may be explained by error in initial mixture composition, uncertainty in temperature, or slight drift in laser center wavelength, etc. Here, all H_2O profiles have been rescaled so that the plateau H_2O concentrations match with the calculated equilibrium levels. Since very dilute mixtures (0.1% O_2) were used in the study, the temperature rise due to exothermicity of the reaction was typically less than 15 K. The change in H_2O absorption cross-section due to the temperature rise is less than 2%. Therefore, the absorption cross-sections of H_2O were treated as constants within each measurement. Shown in Fig. 3 are the H_2O time histories derived from the experimental observations in Fig. 1.

Also shown in Fig. 3 are the best-fit H_2O temporal profiles calculated using GRI-Mech 3.0 and

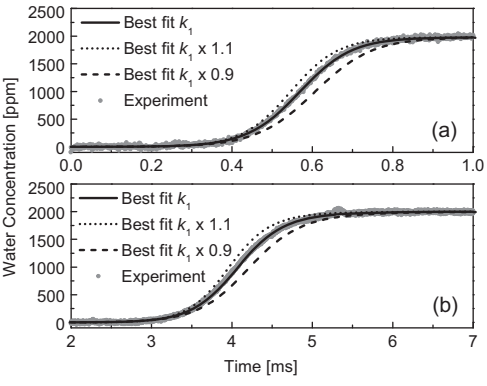

Fig. 3. Comparison of experimental and Senkin calculated H_2O profiles using best-fit k_1 with effect of ±10% variation on k_1 at conditions of the corresponding panels of Fig. 1.

the Senkin kinetics code by varying k_1 to match the maximum slope. Two H_2O profiles calculated using 110% and 90% of the best-fit k_1 are presented for each test. The fitting uncertainty of k_1 is estimated to be ±2%.

To obtain the best-fit in Fig. 3a 0.35 ppm of H atom was artificially included in the mixture used for the numerical simulation to match the onset of the rapid H_2O formation. The addition of H atom simulates the effects of residual contaminants in the shock tube or the mixing tank. It should be noted, however, that the maximum slope of the H_2O profile, which is selected as the criteria for determining k_1 in this study, is not affected by the inclusion of this H atom addition, since the maximum slope is "determined at a point in reaction progress where memory of the initial process is lost" [14]. Numerical calculations confirmed this assumption. The levels of H atoms artificially included for Senkin calculations were found to decrease almost exponentially as the test temperature drops. The H atom concentration needed to match the onset of the H_2O profile in Fig. 3b (1100 K) was only 0.0012 ppm.

H_2O sensitivity analyses in Fig. 2 provide rough estimations of the relative significance of the interfering reactions to reaction (1). To quantitatively evaluate the uncertainty of k_1 introduced by all error sources, sensitivity analyses of the selected criteria, i.e. the maximum slope of H_2O profile, were conducted. Each error source was disturbed by its estimated uncertainty, and k_1 subsequently adjusted to regain the best-fit to experimental data. The percentage change of k_1 is the uncertainty associated with that error term. The maximum slope sensitivities for the conditions of Fig. 1 are demonstrated in Fig. 4, the estimated uncertainty associated with each error source is shown in the parentheses. The estimated uncertainties of the rate coefficients for the interfering reactions are taken from the latest review by Baulch et al. [30]

Figure 4a indicates that at high temperature (1472 K), the approach taken by the present study successfully constrains the uncertainties introduced by interfering reactions. The determination of the reflected shock temperature was found to be the single largest source of uncertainty, at ±3.4%, highlighting the importance of improving the temperature uniformity in the shock tube using the driver insert technique discussed in Section 2. The combined root-sum-square (RSS) of the estimated uncertainties of all sources for k_1 is approximately ±4.6%.

The maximum slope sensitivity analysis of the low temperature experiment (Fig. 4b) indicates that the combined uncertainty of the inferred k_1 is 8.8%. The uncertainty in temperature is again the largest source of error. In addition, at the lower temperatures, some errors are now introduced by interfering reactions, in particular HO_2

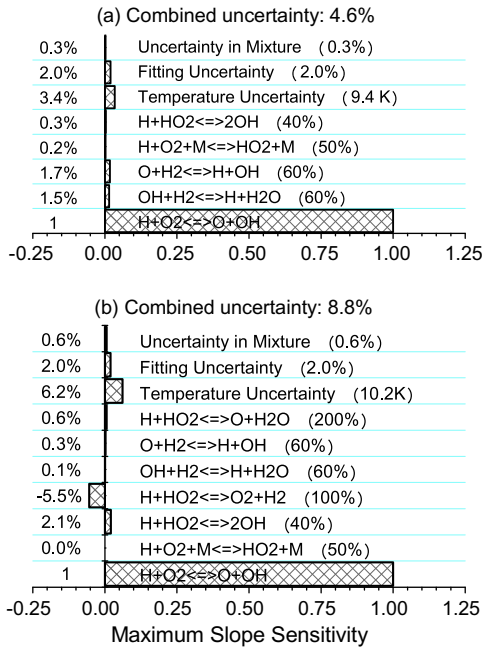

Fig. 4. Sensitivity analyses for the maximum slope of the H_2O profile at the conditions of the corresponding panels of Fig. 1.

reactions. For example, the estimated factor of two uncertainty [30] of the rate coefficient of reaction $H + HO_2 \rightarrow O_2 + H_2$ (k_5) results in a k_1 uncertainty of 5.5%. The uncertainty associated with k_5 is discussed in Section 4. Although H_2O formation shows pronounced sensitivity to reaction $H + O_2 + M \rightarrow HO_2 + M$ (k_2) at low temperature (Fig. 2b), the determination of k_1 is immune to the uncertainty in k_2 by taking the "maximum slope" approach. The quoted k_2 uncertainty in Fig. 4b is taken from Baulch et al. review [30] and takes into account fall-off and third body effects. The selection of k_2 only changes the onset of H_2O formation, which is a similar effect to that of adding small quantities of H-atoms.

The experimental k_1 values are summarized in Fig. 5. A least-squares fit to the current data over the temperature range 1100–1527 K gives $k_1 = (1.12 \pm 0.08) \times 10^{14} \exp[(-7805 \pm 90)/T]\,\mathrm{cm^3\,mol^{-1}\,s^{-1}}$. Presented on the same figure are two sets of experimental data reported by previous researchers [7,9]. Excellent agreement is found between the present study and the study by Masten et al. [9] at the overlapping temperatures. Combining the Masten et al. data with the results from the present study, we obtain an expression $k_1 = (1.04 \pm 0.03) \times 10^{14} \exp[(-7705 \pm 40)/T]\,\mathrm{cm^3\,mol^{-1}\,s^{-1}}$ that is suitable over the temperature range from 1100 to 3370 K, as presented in Fig. 5. In addition, the current data from this study fall completely within the data reported by

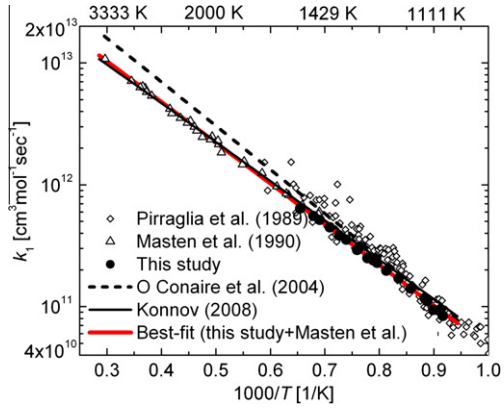

Fig. 5. Arrhenius plot of experimentally determined k_1 from this study and from studies by Pirraglia et al. [7] and by Masten et al. [9]. k_1 values used in two recent chemical kinetic models [31,32] are also shown.

Pirraglia et al. [7], but with much smaller scatter and a slightly different activation energy.

Also shown in Fig. 5 are k_1 expressions used in two recent H_2 combustion mechanisms [31,32]. The rate coefficient k_1 used by Ó Conaire et al. mechanism [31] has a slightly larger activation energy, because the expression was based on the Pirraglia et al. [7] work. Konnov [32] adopted Baulch et al.'s recommendation for k_1 [30], which agrees very well with the experimental data at high temperatures [9] but shows increasing discrepancy with our data at low temperatures. Other recent combustion mechanisms, such as Li et al. H_2 mechanism [33], Saxena and Williams H_2/CO mechanism [34], and GRI-Mech [19]/JetSurF [35], have similar k_1 values to our least-square fit over the entire temperature range between 1100 and 3370 K.

4. Discussion

4.1. Sensitivity of k_1 to k_5

Near the low temperature end of the present study ($T = 1100$ K), one of the interfering reactions $H + HO_2 \rightarrow O_2 + H_2$ (k_5) introduces the second largest uncertainty in k_1. This is partly a result of limited knowledge of k_5 and we have used a factor of two for the uncertainty as assigned in the review by Baulch et al. [30]. Discrepancies of the same order exist among the values of k_5 used in several combustion models [19,31–35]. Once a better understanding of k_5 becomes available, the accuracy of k_1 can be improved.

Figure 6 shows the correlation between k_1 and k_5 at $T = 1100$ K, which is obtained by varying k_5

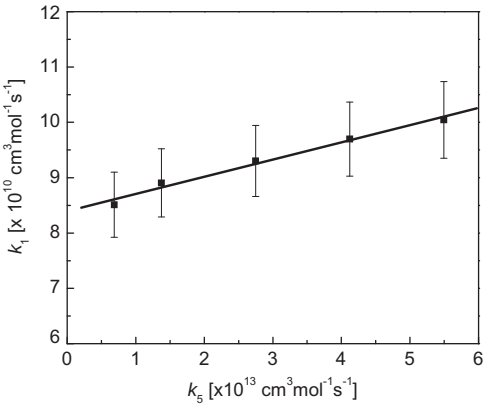

Fig. 6. k_1–k_5 pairs that best-fit the experimental H_2O profile at the conditions of Fig. 1b. The assigned error bar is the combined uncertainty from all error sources except k_5.

in GRI model [19] and subsequently adjusting k_1 to regain the best-fit to the experimental observation. The slope of the line $dk_1/dk_5 = 0.055$, suggesting that the best fit k_1 would increase by 5.5% if k_5 was doubled. The GRI model [19] uses $k_5 = 2.75 \times 10^{13}$ cm^3 mol^{-1} s^{-1} at $T = 1100$ K, while other models use k_5 values ranging from 1.14×10^{13} cm^3 mol^{-1} s^{-1} [31,33,34] to 4.11×10^{13} cm^3 mol^{-1} s^{-1} [32] at the same temperature.

At higher temperatures the sensitivity of our k_1 determination to k_5 decreases rapidly. At temperatures above 1350 K, dk_1/dk_5 is less 1% and can be safely neglected. The analysis also revealed that two different initial H_2 concentrations used in this study do not have an impact on the behavior of dk_1/dk_5.

4.2. Reevaluation of the Masten et al. determination of k_1

The Masten et al. (and other high temperature studies [9–14]) determination of k_1 relied on OH laser absorption experiments. However, $\Delta_f H^\circ_{298}$(OH) was recently revised from 9.40 to 8.91 kcal/mol [22,23], and this change may affect the original k_1 determination.

Masten et al. [9] saw modest differences between the measured and calculated OH plateau values and attributed these to several factors including uncertainty in OH absorption cross-section, and uncertainty in the mixture composition. To avoid these differences they treated the OH profiles as self-calibrating, and always rescaled the experimentally observed OH plateaus to the calculated levels.

Representative data at 1980 and 2898 K from Masten et al. [9] were reanalyzed using the revised OH heat of formation. Although the calculated OH plateau level is different from the experimental data, it can be rescaled as was done by Masten et al. For the 1980 K data, the rescaled OH profile matches well with their experimental data, suggesting that the inferred k_1 was not affected by the update in $\Delta_f H^\circ_{298}$(OH). At 2898 K, a similar analysis shows that k_1 only needs to be increased by 1%, well within the uncertainty of the measurement. Therefore, k_1 values from Masten et al. [9] can be retained.

4.3. Previous studies of k_1 at temperatures below 1500 K

Table 1 summarizes the low-temperature recommendations for k_1 from selected previous studies along with the result from the present study. Two major approaches were taken in the efforts to determine k_1 at temperature below 1500 K: (1) the H-ARAS approach by Pirraglia et al. [7] and by Shin and Michael [8]; and (2) the OH laser absorption approach by Ryu et al. [14] and by Hwang et al. [17]. Discrepancies exist among these studies.

In the analysis of the low concentration ARAS studies, the reaction $H + O_2 + M \rightarrow HO_2 + M$ (k_2), which can be responsible for H atom decay, was neglected in both H-ARAS studies. Recent study has greatly improved understanding of this competing reaction [21]. k_1 values inferred from H-ARAS studies can be reevaluated to account for the error of neglecting k_2. The error associated with neglecting k_2 was estimated to be approximately 7% at one representative test condition reported by Pirraglia et al. ($T = 1098$ K, $P = 0.25$ atm, 1.85% O_2/0.074% NH_3/Ar), which helps to account for the difference between the present study and Pirraglia et al. at 1100 K.

However, the difference between Pirraglia et al. and this study is 21% at $T = 1500$ K, where the influence of k_2 becomes insignificant and can be safely neglected. In addition, we noticed that the discrepancy between both H-ARAS studies [7,8] is significant (about 20% at 1100 K). The substantial discrepancy, as well as the large scatter seen in the H-ARAS studies, may be attributed to photolytes used to generate H radicals. Pirraglia et al. found that k_1 values using the H_2O photolyte were consistently larger (by 60%) than the results using NH_3 as the photolyte. They also observed unusually low initial H atom concentrations and large errors associated with the H_2O photolyte [7], and therefore excluded the H_2O photolyte data in the final expression of k_1. Shin and Michael [8] also observed that the H_2O photolyte resulted in higher k_1 values over the entire experimental temperature range by 20%. However, they decided to include the H_2O-photolyte data in their final expression since the possible systematic difference (20%) was smaller than the experimental scatter (27%).

Ryu et al. [14] extended the measurements of k_1 to temperatures as low as 1050 K using OH

Table 1
Low temperature reaction rate coefficient k_1 in the form $k_1 = AT^n\exp(-\Theta/T)$.

A ($cm^3\ mol^{-1}\ s^{-1}\ K^{-n}$)	n	Θ (K)	T range (K)	Reference
1.2×10^{14}		8101	1000–2500	Pamidimukkala et al. [4]
$(1.68 \pm 0.19) \times 10^{14}$		8119 ± 139	960–1710	Pirraglia et al. [7]
$(6.93 \pm 0.96) \times 10^{13}$		6917 ± 193	1103–2055	Shin and Michael [8]
1.59×10^{17}	−0.927	8493	1050–2700	Yuan et al. [10]
$(7.13 \pm 0.31) \times 10^{13}$		7065 ± 140	1050–2500	Ryu et al. [14]
6.73×10^{15}	−0.50	8390	950–3100	Hwang et al. [17]
$(1.12 \pm 0.08) \times 10^{14}$		7805 ± 90	1100–1527	This study
$(1.04 \pm 0.03) \times 10^{14}$		7705 ± 40	1100–3370	This study + Masten et al. [9]

laser absorption. Test mixtures of high concentration (4% H_2/1% O_2/Ar) had to be employed to compensate for the low OH yield at low temperatures. Calculation with the GRI model [19] shows that the temperature rise is approximately 180 K when the OH peak concentration is reached, or 370 K when oxidation is completed with the concentration stated in the reference. Other factors, such as the temperature dependency of the OH absorption coefficient, and more pronounced impacts from interfering reactions, may contribute to the difference between the H-ARAS [7] and the OH [14] approaches. To reconcile the discrepancy, Hwang et al. [17] used the OH diagnostic to reinvestigate the reaction. Although mixtures with high H_2 and O_2 concentrations were used in their study to evaluate k_1 at low temperatures, temperature profiles were continuously updated using experimentally recorded pressure profiles during the course of reaction, and the corrected OH time-histories were fitted using comprehensive computer simulations. The low-temperature ($T < 1500$ K) results of Hwang et al. [17] support the previous H-ARAS study [7] and have excellent agreement with the current study (within 6% at 1100 K).

Miller et al. [36] proposed a rate expression for k_1 (1.98×10^{14} $(T/1000)^{-0.591}$ $\exp(-8152/T)$ [$cm^3\ mol^{-1}\ s^{-1}$]) by combining the equilibrium constant of the reaction and the reverse rate constant from theoretical studies. Their expression utilizes an activation energy identical to ΔH°_0 of the reaction. Using the same approach and best-fitting the current data and those of Masten et al. [9], we obtained a 3-parameter expression $k_1 = 1.58 \times 10^{14}$ $(T/1000)^{-0.262}$ $\exp(-8152/T)$ [$cm^3\ mol^{-1}\ s^{-1}$] over the temperature range from 1100 to 3370 K. The standard deviation for $\ln(k_1)$ of this 3-parameter fit is 0.04, which is identical to that of the 2-parameter expression proposed in Section 3, and therefore can be used as an alternative for combustion modeling.

5. Conclusions

Very dilute fuel-rich H_2/O_2 mixtures were shock-heated to temperatures between 1100 and 1532 K to study the rate coefficient of the branching reaction $H + O_2 \rightarrow OH + O$ (k_1). Using tunable diode laser absorption of H_2O near 2.5 μm, H_2O time-histories were recorded. The rate coefficients of the reaction were determined by varying k_1 in GRI-Mech 3.0 to generate H_2O profiles that best-fit the experimental observations. The results are well-fit by $k_1 = (1.12 \pm 0.08) \times 10^{14}$ $\exp[(-7805 \pm 90)/T]$ $cm^3\ mol^{-1}\ s^{-1}$, with estimated uncertainties of 4.6% at 1500 K and 8.8% at 1100 K.

The determinations of k_1 from previous OH laser absorption studies were reevaluated using the updated OH enthalpy of formation and the results in the literature were found to be unaffected. Excellent agreement between this study and that of Masten et al. (1990) was found at the overlapping temperatures. By combining the results of the two studies, we recommend the expression $k_1 = (1.04 \pm 0.03) \times 10^{14}$ $\exp[(-7705 \pm 40)/T]$ $cm^3\ mol^{-1}\ s^{-1}$ over the temperature range from 1100 to 3370 K. At temperatures below 1500 K, the good agreement was found between the present study and that by Pirraglia et al. [7]. In addition, excellent agreement (within 6% over 1100–1500 K) was found between the present study and the recent OH measurements by Hwang et al. [17].

Acknowledgements

The authors thank Profs. C.T. Bowman and D.M. Golden from Stanford University for many useful discussions. This work was supported by the National Science Foundation under Award Number CBET-0649936 and by the Department of Energy [National Nuclear Security Administration] under Award Number NA28614.

Appendix A. Supplementary data

Supplementary data associated with this article can be found, in the online version, at doi:10.1016/j.proci.2010.05.101.

References

[1] C.K. Westbrook, F.L. Dryer, *Prog. Energy Combust. Sci.* 10 (1984) 1–56.

[2] D.L. Baulch, D.D. Drysdale, D.G. Horne, A.C. Lloyd*Evaluated Kinetic Data for High Temperature Reactions*, vol. 1, Butterworth, London, 1972.

[3] G.L. Schott, *Combust. Flame* 21 (1973) 357–370.

[4] K.A. Pamidimukkala, G.B. Skinner, in: Thirteenth International Symposium on Shock Waves and Shock Tubes, Suny, Albany, 1981, pp. 585–592.

[5] P. Frank, T. Just, *Ber. Bunsenges. Phys. Chem.* 89 (1985) 181–187.

[6] N. Fujii, K.S. Shin, *Chem. Phys. Lett.* 151 (1988) 461–465.

[7] A.N. Pirraglia, J.V. Michael, J.W. Sutherland, R.B. Klemm, *J. Phys. Chem.* 93 (1989) 282–291.

[8] K.S. Shin, J.V. Michael, *J. Chem. Phys.* 95 (1991) 262–273.

[9] D.A. Masten, R.K. Hanson, C.T. Bowman, *J. Phys. Chem.* 94 (1990) 7119–7128.

[10] T. Yuan, C. Wang, C.-L. Yu, M. Frenklach, M.J. Rabinowitz, *J. Phys. Chem.* 95 (1991) 1258–1265.

[11] H. Du, J.P. Hessler, *J. Chem. Phys.* 96 (1991) 1077–1092.

[12] H. Yang, W.C. Gardiner, K.S. Shin, N. Fujii, *Chem. Phys. Lett.* 231 (1994) 449–453.

[13] C.-L. Yu, M. Frenklach, D.A. Masten, R.K. Hanson, C.T. Bowman, *J. Phys. Chem.* 98 (1994) 4770–4771.

[14] S. Ryu, S.M. Hwang, M.J. Rabinowitz, *J. Phys. Chem.* 99 (1995) 13984–13991.

[15] J. Warnatz, in: W.C. Gardiner (Ed.), *Combustion Chemistry*, Springer Verlag, New York, 1984.

[16] N. Cohen, K.R. Westberg, *J. Phys. Chem. Ref. Data* 12 (1983) 531–590.

[17] S.M. Hwang, Si-Ok Ryu, K.J. De Witt, M.J. Rabinowitz, *Chem. Phys. Lett.* 408 (2005) 107–111.

[18] Z. Hong, A. Farooq, E.A. Barbour, D.F. Davidson, R.K. Hanson, *J. Phys. Chem. A* 113 (2009) 12919–12925.

[19] G.P. Smith, D.M. Golden, M. Frenklach, et al., available at. <http://www.me.berkeley.edu/gri-mech/>

[20] A.E. Lutz, R.J. Kee, J.A. Miller, Senkin: A FORTRAN Program for Predicting Homogeneous Gas Phase Chemical Kinetics with Sensitivity Analysis, Report No. SAND87-8248, Sandia National Laboratory, 1988.

[21] R.X. Fernandes, K. Luther, J. Troe, V.G. Ushakov, *Phys. Chem. Chem. Phys.* 10 (2008) 4313–4321.

[22] J.T. Herbon, R.K. Hanson, D.M. Golden, C.T. Bowman, *Proc. Combust. Inst.* 29 (2003) 1201–1208.

[23] B. Ruscic, A.F. Wagner, L.B. Harding, et al., *J. Phys. Chem. A* 106 (2002) 2727–2747.

[24] J.T. Herbon, Shock Tube Measurements of $CH_3 + O_2$ Kinetics and the Heat of Formation of the OH Radical, PhD Thesis, Stanford University, 2004, Available at <http://thermosciences.stanford.edu/pdf/TSD-153.pdf>.

[25] Z. Hong, G.A. Pang, S.S. Vasu, D.F. Davidson, R.K. Hanson, *Shock Waves* 19 (2009) 113–123.

[26] A. Goldman, R.R. Gamache, A. Perrin, J.M. Flaud, C.P. Rinsland, L.S. Rothman, *J. Quant. Spectrosc. Radiat. Transfer* 66 (2000) 455–486.

[27] Z. Hong, S.S. Vasu, D.F. Davidson, R.K. Hanson, *J. Phys. Chem. A* 114 (2010) 5520–5525.

[28] Z. Hong, R.D. Cook, D.F. Davidson, R.K. Hanson, *J. Phys. Chem. A* 114 (2010) 5718–5727.

[29] B. Ruscic, R.E. Pinzon, M.E. Morton, N.K. Srinivasan, M.-C. Su, J.W. Sutherland, J.V. Michael, *J. Phys. Chem. A* 110 (2006) 6592–6601.

[30] D.L. Baulch, C.T. Bowman, C.J. Cobos, et al., *J. Phys. Chem. Ref. Data* 34 (2005) 757–1397.

[31] M. Ó Conaire, H.J. Curran, J.M. Simmie, W.J. Pitz, C.K. Westbrook, *Int. J. Chem. Kinet.* 36 (2004) 603–622.

[32] A.A. Konnov, *Combust. Flame* 152 (2008) 507–528.

[33] J. Li, Z. Zhao, A. Kazakov, F.L. Dryer, *Int. J. Chem. Kinet.* 36 (2004) 566–575.

[34] P. Saxena, F.A. Williams, *Combust. Flame* 145 (2006) 316–323.

[35] B. Sirjean, E. Dames, D.A. Sheen, et al., available at <http://melchior.usc.edu/JetSurF/Version0_2/Index.html>.

[36] J.A. Miller, M.J. Pilling, J. Troe, *Proc. Combust. Inst.* 30 (2005) 43–88.